ARTICLES

Probing Förster and Dexter Energy-Transfer Mechanisms in Fluorescent Conjugated Polymer Chemosensors

Clifford B. Murphy,[†] Yan Zhang,[†] Thomas Troxler,[‡] Vivian Ferry,[†] Justin J. Martin,[†] and Wayne E. Jones, Jr.*[,†]

Department of Chemistry and Institute for Materials Research, State University of New York at Binghamton, Vestal Parkway East, Binghamton, New York 13902, and NIH Regional Laser and Biotechnology Laboratory, University of Pennsylvania, Philadelphia, Pennsylvania 19104

Received: January 31, 2003; In Final Form: October 7, 2003

Fluorescence quenching in solutions of a pendant-functionalized conjugated polymer chemosensor (**ttp-PPETE**) has been evaluated in the presence of a variety of transition metal cations, including Ni^{2+}, Co^{2+}, Cu^{2+}, Fe^{2+}, and Cr^{6+}. Photophysical analysis of the emission quenching revealed a static quenching mechanism that demonstrated strong positive deviations from predicted linear behavior. The enhanced emission quenching mechanism was found to correlate closely with the relative loading of the cationic analytes on the polymer chemosensor. This behavior has been attributed to rapid energy transfer along the polymer backbone. A modified Stern−Volmer static quenching model has been successfully applied that incorporates an energy-transfer term that takes into account different energy-transfer mechanisms. Both Förster and Dexter energy-transfer enhancements were observed for **ttp-PPETE** quenching depending upon the identity of the quencher analyte involved. Stern−Volmer constants in all cases were on the order of 10^5 M^{-1} for the transition metals reported. Photophysical characterization for **ttp-PPETE** includes absorbance, emission, and single-photon counting lifetimes in the absence and presence of varying concentrations of the analytes.

Introduction

Fluorescent conjugated polymers have enjoyed a great deal of attention in recent years as chemosensory materials[1] for a wide array of analytes from explosives and biomolecules to toxic transition metal ions.[2] The basis for this is due in part to predicted signal enhancement over similarly structured small molecule sensors as a result of exciton delocalization and rapid energy transfer along the polymeric backbone.[3] Depending on the receptor functionality and its placement within the polymer structure, low analyte concentrations can be detected as ionochromic shifts,[4,5] potentiometric fluctuations,[5a,6] and increased[7] or far more commonly decreased luminescence intensity.[1−3,8,9] Emission quenching in these polymeric chemosensors is characterized by very large quenching constants.[8] Regardless of the means of detection, desirable chemosensory materials must demonstrate sensitivity to analytes, as well as specificity with which to distinguish between analytes and possible interferents.

Our interest in these polymers[10−12] is the design of new materials suitable for use in portable chemosensory devices for rapid, accurate field analysis of select transition metal ion contaminants in aqueous waste streams as identified by the EPA[13] and target contaminants of Superfund[14] cleanup sites. We have previously described the synthesis of a series of pendant functionalized conjugated polymer chemosensors[10,11] and demonstrated their potential application to an array sensory system.[12] These poly(phenylene ethynylene thienylene ethynylene) polymers are known to have high fluorescent quantum yields,[15,16] and by appending a Lewis base receptor ligand such as tolylterpyridine[17] (**ttp-PPETE**, Chart 1) in conjugation with the polymer backbone, we demonstrated significant fluorescence quenching with transition metal cations.[10−12] A single binding event results in quenching the fluorescence from several repeat units along the polymer backbone. This is due to energy transfer

CHART 1: Structures of PPETE and ttp-PPETE Polymers

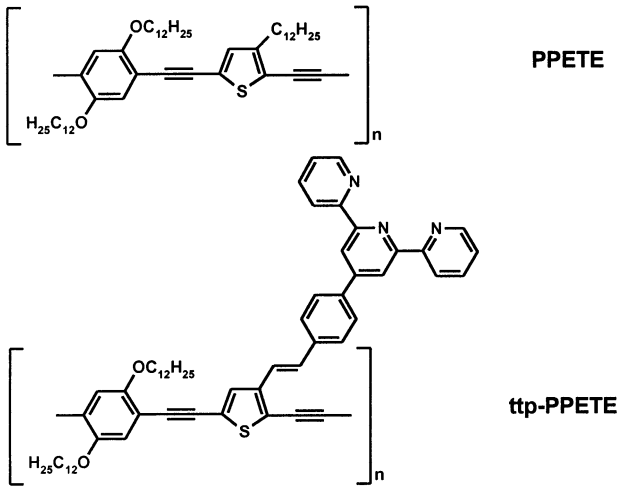

* Author to whom correspondence should be sent. E-mail: wjones@binghamton.edu. Phone: (607)-777-2421. Fax: (607)-777-4478.
[†] State University of New York at Binghamton.
[‡] University of Pennsylvania.

10.1021/jp0301406 CCC: $27.50
Published on Web 01/10/2004

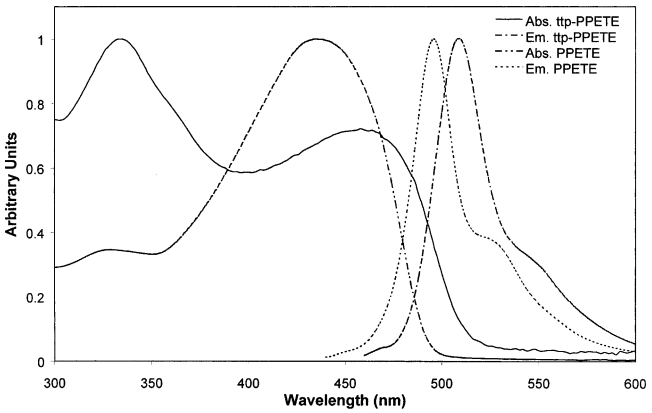

Figure 1. Normalized absorbance and emission profiles for **PPETE** and **ttp-PPETE** polymers in THF.

from nonbound sites to quencher bound repeat units, yielding large quenching constants as determined by Stern−Volmer analysis.

A better understanding of energy-transfer processes in conjugated polymer sensors would provide critical information for the interpretation of increased quenching selectivity and the design of new, more sensitive, chemosensory materials. Collisional quenching interpreted via Stern−Volmer analysis has long been used to probe energy transfer along polymer backbones[18,19] and between pendant chromophores such as carbazole.[20] These studies have been able to determine energy-transfer parameters such as the rate of transfer, rate of migration, Förster critical distance, etc., with the application of random walk and continuous energy migration models.[21,22] A review in the literature puts these models and techniques to use in the context of photon-harvesting polymers.[23] However, some limitations have been noted for these methods in that energy transfer may not be observable, or may in fact reduce rather than increase observed quenching.[24] Typically linear Stern−Volmer plots for polymer systems demonstrate curvature in those instances where energy-transfer processes have been observed. This leads to very high quenching constants. These phenomena have been described in the literature as "superquenching" of polymer flurophores.[8c,25]

In this paper we probe the photophysics of the **ttp-PPETE** polymer system and its quenching interactions with Ni^{2+}, Co^{2+}, Cu^{2+}, Cr^{6+}, and Fe^{2+} in solution. Stern−Volmer analysis for these polymers demonstrates a static (complexational) quenching mechanism, which shows a positive curvature away from predicted linear behavior. Herein we describe the observed quenching mathematically by modifying the static Stern−Volmer quenching expression to incorporate a term to account for nonradiative energy-transfer processes. This term takes a different form depending on the energy-transfer mechanism involved, prompting an observation of either Dexter or Förster mechanisms depending on the identity of the quenching analyte. To the best of our knowledge, this is the first demonstration of this mathematical model applied to polymer quenching and of tuning the energy-transfer mechanisms in a polymer through analyte loading.

Experimental Section

Materials. All materials were purchased from Aldrich and used as received unless otherwise noted. The synthesis and characterization of poly-2,5-didodecyloxyphenylene ethynylene 3-*trans*-(((4′-*p*-phenyl)-2,2′:6,2″-terpyridine)-vinylene)-thiophene ethynylene (**ttp-PPETE**, Chart 1) has been reported previously.[11] Metallic salts used for making metal ion parent solutions include $NiCl_2 \cdot 6H_2O$, $CoCl_2 \cdot 6H_2O$, $CuCl_2 \cdot 2H_2O$, and $FeSO_4 \cdot 7H_2O$. Chromium(VI) quenching solutions used the Aldrich atomic absorption standard solution (Cat. No. 29,204-4) as the metallic ion parent solution.

Sample Preparation. All samples for UV−vis, fluorimetry, and single-photon counting experiments were prepared as dilute THF solutions, and protected from ambient light until use. Polymer stock solution with a 5.0×10^{-6} M concentration by monomer-unit weight was prepared, resulting in an optical density of ~0.1 at $\lambda = 410$ nm. Metal stock solutions were prepared at 2.50×10^{-4} M concentration in distilled water. Solutions for emission quenching experiments were prepared via titration, pipetting 25- or 50-μL aliquots of metal solution into 50 mL of polymer solution with THF as solvent. All sample solutions were studied under ambient atmospheric conditions within 4 h of initial preparation.

Photophysics. UV−vis absorbance spectra were taken on a HP 8253A diode-array spectrometer from 190 to 820 nm or a Perkin-Elmer double beam Lambda 2 spectrometer from 300 to 700 nm. Emission spectra were acquired on an SLM 48000s fluorimeter with 410-nm excitation from a 450-W Xenon lamp through 4-nm slits. Emission was collected 90° relative to excitation through 4-nm slits. Absorbance and fluorescence were observed in a quartz cuvette with a 1.0-cm path length. I_0/I data for Stern-Volmer analysis was corrected for any changes in absorbance at $\lambda = 410$ nm.

Time-Resolved Emission. The fluorescence decay kinetics were determined by time-correlated single photon counting. The system, housed at the NIH Regional Laser and Biotechnology Laboratories at the University of Pennsylvania, has been described in detail elsewhere.[26] The laser system consists of a mode-locked Nd:YAG laser (Coherent Antares) synchronously pumping a home-built, single-jet, cavity dumped dye laser, operating at 3.8 MHz. Doubling the output of the dye laser (LDS 751 dye in propylene carbonate/ethylene glycol) provided excitation at 375 nm in a $LiIO_4$ crystal. Fluorescence was collected at 90° relative to excitation, with emission polarized at the magic angle (54.7°), dispersed by a double monochromator in subtractive dispersive mode and detected at 510 nm by a microchannel-plate photomultiplier tube (Hamamatsu R3809U). The spectral bandwidth for the instrument was typically 15 nm, and its overall time resolution was determined to be 35 ps. The fluorescence decay data were analyzed by nonlinear least-squares fits of individual traces with the program LIFETIME.[26a] It was assumed that each decay curve was comprised of a sum of single exponentials. This program also convolutes the instrument response curve into the sample decay data prior to fitting. Samples were prepared in a similar manner as described for the solutions in the emission series.

Stern−Volmer Curve Fitting. Curve fitting and data analysis of the Stern−Volmer quenching relationships were completed in Microsoft Excel 2000, using the Solver plug-in application, and minimizing the sum of the square of the residuals.[27]

Results and Discussion

Polymer Photophysics. The high quantum yield fluorescence of the polyarylene ethynylene conjugated polymers makes them ideal candidates for fluorescent chemosensory materials. The general photophysical properties of this class of materials have been reviewed.[16] Recently, we have extended the photophysics to include results for substituted **PPETE** systems. **PPETE** was chosen as the backbone for our chemosensor polymer as it is known to have a high ϕ_f (~0.4 in THF)[15] and the emission appears in the visible region as bright green ($\lambda_{max} \sim 498$ nm)

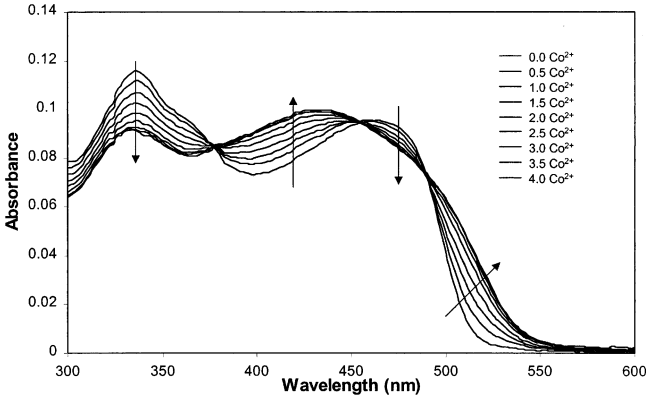

Figure 2. Absorbance series for 5.00×10^{-6} M **ttp-PPETE** in THF titrated with increasing concentrations of Co^{2+} ($\times 10^{-6}$ M) ions.

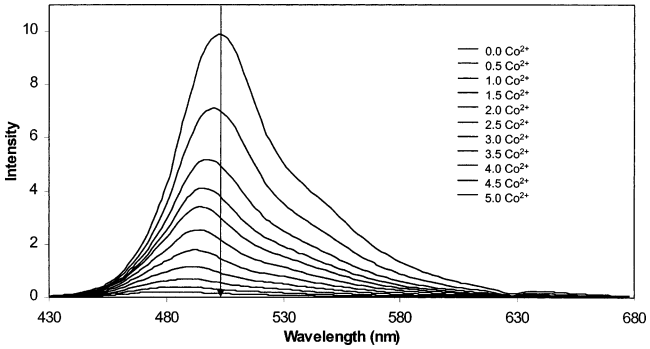

Figure 3. Emission quenching of 5.00×10^{-6} M **ttp-PPETE** by increasing concentrations of Co^{2+} ($\times 10^{-6}$ M) ions, $\lambda_{ex} = 410$ nm. The solid arrow indicates the blue-shift in emission maxima with increased quencher ion concentrations.

to the naked eye. The $\pi-\pi^*$ bands absorb across a large region of blue and violet into the ultra-violet regions of the spectrum with a Stokes shift of the emission into the visible region of the spectrum. This makes it easy to excite into the emissive state without interfering with the emission signal. Typical absorbance spectra for the **PPETE** and **ttp-PPETE** systems in THF solution are shown in Figure 1 and compare favorably with literature results,[15] taking into account differences in alkoxy chain lengths. The **PPETE** model backbone (where both R and R′ are alkyl chains) has a strong absorbance maximum around 440 nm and a weaker absorbance at 325 nm. Both of these transitions have previously been assigned to $\pi-\pi^*$ transitions in the conjugation of the polymer backbone. The terpyridine-pendant polymer (**ttp-PPETE)** exhibits an additional strong absorbance at 340 nm consistent with the absorption that is observed for the $\pi-\pi^*$ transition in the tolylterpyridyl monomer. Upon addition of the pendant terpyridyl group a distinct red shift is observed for the lowest energy relative to the model **PPETE** backbone ($\lambda_{max} = 460$ nm). This shift is consistent with an increase in the overall conjugation along the backbone as expected.

The addition of transition metal ions to solutions of **ttp-PPETE** results in subtle shifts to the observed absorbance spectra and no change in the absorbance for solutions of the model polymer, **PPETE**. Representative absorbance spectra for the polymer−metal ion systems are shown for the interaction of **ttp-PPETE** with Co^{2+} in Figure 2. With increased metal ion concentration, the terpyridyl band decreases in intensity while the lowest energy transition exhibits a pronounced broadening along with a slight blue-shift in energy. This is true to varying degrees for all of the metal ions tested here, including Ni^{2+}, Cu^{2+}, Fe^{2+}, Cr^{6+}, and Co^{2+}.

Emission spectra for the **PPETE** and **ttp-PPETE** (Figure 1) polymers have been shown previously to originate from the lowest energy $\pi-\pi^*$ excited state on the **PPETE** backbone.[10,11] The room temperature emission of **ttp-PPETE** shows a sharp maxima at 508 nm and a broader shoulder at 550 nm. By comparison to model systems, the emission originates from the polymer backbone with a red-shift for **ttp-PPETE** relative to **PPETE**, consistent with increased conjugation suggested by the absorbance data.

Emission Quenching. In the presence of the terpyridyl receptor, luminescence quenching of our polymer system was observed for solutions containing several different metal ions. Previously we have reported nM sensitivity of the polymer fluorescence to nickel(II) cations in solution.[10] While this system is highly selective for Ni^{2+}, quenching is also observed for Co^{2+}, Cu^{2+}, Fe^{2+}, and Cr^{6+} cations in solution. A representative spectral series for Co^{2+} is shown in Figure 3. In the case of Co^{2+}, the polymer is quenched and the emission undergoes a slight blue-shift of up to 10 nm with increasing transition metal ion concentration. Similar behavior is observed with the other transition metals tested, with variation in the total quenching efficiency observed in each case. This behavior of the **ttp-PPETE** chemosensor system is outlined in further detail below.

TABLE 1: Biexponential Lifetimes for 3.00×10^{-6} M ttp-PPETE Solutions in THF by Single-Photon Counting

[analyte] ($\times 10^{-7}$ M)	$\tau_f^{a,b,c}$ (ns)
0	0.53 (0.50), 0.13 (0.50)
5.00 Ni^{2+}	0.57 (0.48), 0.14 (0.52)
5.00 Co^{2+}	0.59 (0.52), 0.20 (0.48)
5.00 Cr^{6+}	0.67 (0.50), 0.19 (0.50)

[a] $\lambda_{ex} = 410$ nm, $\lambda_{em} = 510$ nm. [b] Component contribution in parentheses. [c] Lifetimes accurate to ±0.04 ns.

Emission lifetimes were evaluated by single-photon counting at 410-nm excitation. Decays were best fit by a standard biexponential decay as shown in Table 1. Lifetimes for both decay components in the polymer samples are longer in the presence of metal ions in all cases, indicative of some change in the emissive state. The magnitude of each lifetime component, τ_1 and τ_2, was independent of the presence or identity of the metallic ions evaluated here. Under all experimental conditions, the long component of the lifetime remains around 550 ps, though the shorter component varies from 130 to 200 ps depending on the transition metal quencher. The free and metalated **ttp-PPETE** solutions were compared under 410-nm illumination, which excites primarily into the backbone $\pi-\pi^*$ transition, Figure 2. In the presence of metal ions, the **ttp-PPETE** lifetime remained biexponential with only small shifts in each lifetime component.

Stern−Volmer Analysis. The nature of the quenching process in **ttp-PPETE** was probed by Stern−Volmer analysis. Stern−Volmer plots are a useful method of presenting data on emission quenching. From these data the dynamic or static nature of the quenching processes can be determined. In this analysis, the relative lifetimes (τ, τ^0) or intensity (I, I^0) are plotted vs concentration of quencher ions [Q], according to eq 1. The slope of the line is equivalent to k_d, the rate of dynamic

$$\tau_0/\tau \text{ or } I_0/I = 1 + k_d[Q] \quad (1)$$

quenching.[28] Dynamic quenching involves deactivation of the polymer exciton through collisions with quencher molecules or

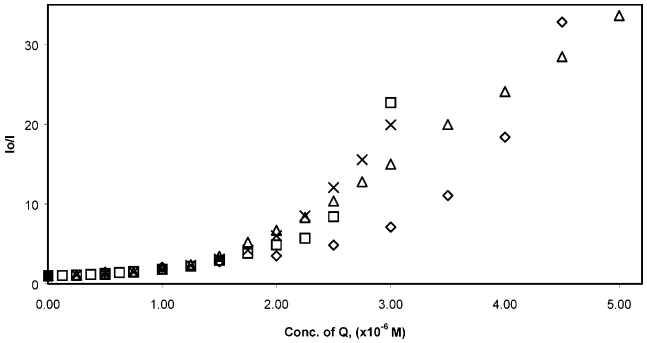

Figure 4. Stern−Volmer plots for the quenching of 5.00×10^{-6} M **ttp-PPETE** by Co^{2+} (diamonds), Cu^{2+} (squares), Fe^{2+} (triangles), and Ni^{2+} (asterisks).

ions in solution. When present, one can determine the rate of quenching, k_q, from the slope of the Stern−Volmer plot and the lifetime ($k_d = k_q\tau_D$). Conversely, static quenching results from complexation of the analyte to the receptor sites, creating new absorption, relaxation, or energy-transfer processes that favor nonradiative decay or evolving into a new excitation/emission behavior. Analysis of Stern−Volmer plots in this regime yields equilibrium expressions for static quenching, K_{SV}, which are analogous to associative binding constants for the quencher−acceptor system.

In a lifetime-based Stern−Volmer plot, when k_d is positive, the quenching is considered dynamic. When k_d is zero, no dynamic quenching can be measured, and emission is quenched by a static mechanism. The lifetime data observed for **ttp-PPETE** in the presence of transition metal ions (Table 1) are invariant within experimental limitations. We conclude that for the **ttp-PPETE** polymer a static quenching mechanism is in effect.

Plotting relative emission intensities (I, I^0) against quencher concentration [Q] for static processes should yield a linear Stern−Volmer plot that describes the static quenching process. Expressed as eq 2, the slope of this plotted line yields K_{SV}, the static quenching constant or associative equilibrium constant.[28] Figure 4 shows the steady-state emission Stern−Volmer analysis

$$I_0/I = 1 + K_{SV}[Q] \qquad (2)$$

for each metal−polymer interaction in THF solution, plotted as in eq 2. These data for Ni^{2+}, Co^{2+}, Cu^{2+}, and Fe^{2+} show very strong quenching from solutions of **ttp-PPETE**, with Ni^{2+} inducing the strongest response. In all cases nonlinear behavior that shows a positive deviation from the typically linear Stern−Volmer analysis was observed.

Aggregation and Conformation. A key question raised by the Stern−Volmer analysis involves the role that aggregation and intramolecular polymer conformation have in the observed nonlinear quenching behavior. While the optical experiments described above were completed at extremely low concentrations (10^{-8} M in polymer), it is possible that intra- and intermolecular interactions may exist. Coordination-driven aggregation where two receptor sites, either both on the same polymer chain or from two different polymer chains, bind to a single metal quencher was of particular concern. To rule out this type of multiple receptor site coordination, experiments with monoterpyridal metal complexes[29] interacting with our chemosensory polymers were undertaken. Initial experiments with the Ni(tpy)Cl_2 complex demonstrate Stern−Volmer quenching with positive curvature nearly identical with that observed with solvated Ni^{2+} ions.[30] This result suggests that the observed curvature is due to a different mechanism.

To explore the behavior exhibited by **ttp-PPETE**, light-scattering and viscosimetry were examined. The goal of this effort was to distinguish between aggregation, conformational changes, and/or energy transfer as contributors to the observed nonlinear behavior. Several experiments were conducted in THF, with polymer concentrations of 1.0 ± 0.2 mg/mL. It should be noted that such concentrations are near the solubility limit for our polymers. No significant change in the low-angle light-scattering intensity or the overall solution viscosity was observed. This suggests that no gross changes in polymer mass or volume have occurred with the addition of transition metal analytes to polymer solutions in THF.

Energy-Transfer Enhanced Stern−Volmer Analysis. A significant difference in quenching behavior has long been noted for polymers, where energy transfer along the polymer backbone is possible. Several modifications to the Stern−Volmer equation have been described in the literature to take into account deviations from linear Stern−Volmer quenching. Common modifications include combinations of dynamic and static mechanisms to the quenching process,[28] or other more detailed manipulations based on hypothesized quenching mechanisms.[8−9,21,24,25]

In recent literature, Whitten and co-workers characterized a functionalized polyphenylene vinylene polymer system, MEH-PPV, as having a millionfold enhancement in quenching sensitivity to methyl viologen relative to a similarly structured *trans*-stilbene molecule.[8a] This behavior was fit with a sphere-of-action adapted Stern−Volmer equation, which was further modified to account for electrostatic concerns native to the specific quencher−sensor combination being investigated.[9a,b] The sphere-of-action model modifies the typical dynamic quenching equation for high relative concentrations of quencher ions to accommodate the high probability of a quenching collision within the lifetime of the excited state.[28] Though the sphere-of-action model does support an upward curvature, this method was inappropriate for the **ttp-PPETE** system as it requires a dynamic quenching component rather than the static quenching mechanism as found in most receptor-based sensors.

Increased sensitivity in the **ttp-PPETE** system was expected to arise from energy transfer along the backbone. Energy-transfer enhancements to emission quenching have long been known for dynamic quenching systems.[18−20] Mechanistic models typically break down the experimentally determined dynamic quenching rate, k_d, into a combination of the rate of quenching (k_Q) and the monomer-to-monomer energy-transfer rate (k_{ET}). Limitations to these methods were described by Webber et al., based on the relative rates of quencher collisions, excitation quenching, and energy transfer.[24] These processes can be described for dynamic and static quenching mechanisms as shown graphically in Figure 5. In Figure 5, k_{diff} refers to the rate of quencher diffusion in solution. In a situation where quenchers are exchanging slowly relative to the rates of energy transfer and quenching ($k_{diff} \ll k_Q$, k_{ET}), the quencher is essentially resident on the polymer. If the rate of energy transfer is limiting relative to that for quenching ($k_{diff} \ll k_{ET} < k_Q$), energy-transfer-enhanced quenching should be observed as the excitation energy migrates along the polymer backbone to the quenched site where it is nonradiatively deactivated. In our system, static quenching observed for the **ttp-PPETE** polymer satisfies the slow diffusing quencher requirement ($k_{diff} \approx 0$) of Webber's stipulations for dynamic systems.

In the presence of significant energy transfer, a loading dependence of quenchers onto the polymer should exist that is independent of the concentration of polymer in solution. This loading dependence is a result of the expressions for quencher

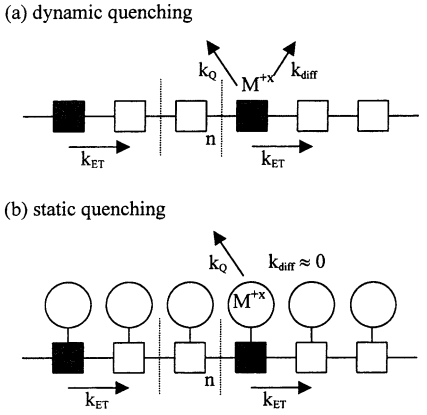

Figure 5. Representation of processes leading to energy-tranfer enhanced quenching for (a) dynamic (adapted from ref 24) and (b) static quenching mechanisms.

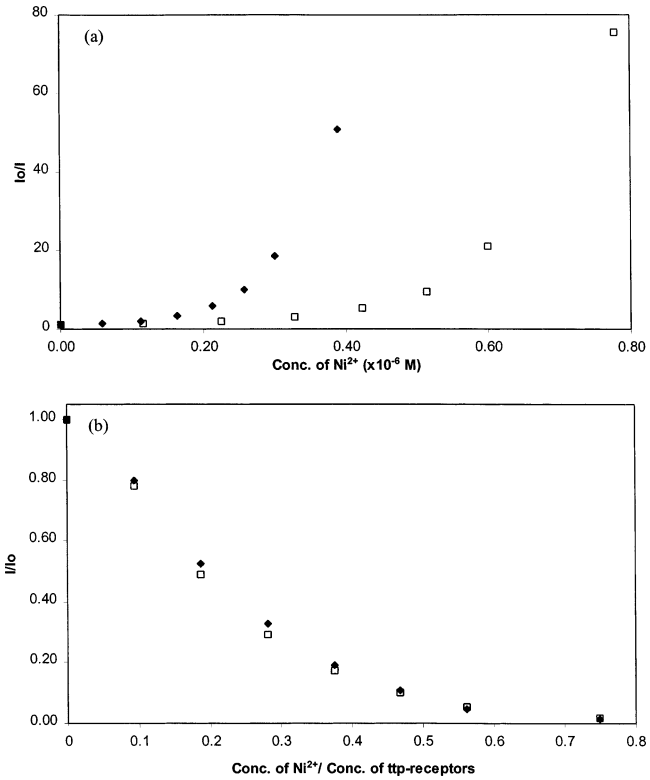

Figure 6. (a) Concentration dependence of Stern−Volmer quenching of **ttp-PPETE** by increased concentrations of Ni^{2+} ions; (b) replot of data from part a to illustrate the loading dependence of fluorescence quenching. Diamonds represent quenching data for 4.00×10^{-6} M **ttp-PPETE**, and squares represent quenching data for 8.00×10^{-6} M **ttp-PPETE**.

encounter probability as put forth for an infinite chain theoretical model by Lakatos-Lindenberg et al. in 1972.[21] In Figure 6a we show the Stern−Volmer analysis of 4.00×10^{-6} and 8.00×10^{-6} M **ttp-PPETE** (by monomer weight) in THF as quenched by Ni^{2+} ions. The positive deviation from linearity occurred at roughly twice the quencher concentration in the more concentrated polymer sample. Replotting these data as I/I_0 against the relative loading of quencher ions ([Q]/[receptors]), a clear overlap of the emission quenching profile is observed, indicative of a reproducible loading dependence, as shown in Figure 6b.

These observations have led us to develop a new model to describe fluorescence quenching in our polymer systems. This model takes the form of an energy-transfer-enhanced Stern−Volmer equation as shown in eq 3, and is consistent with the theoretical models described above. We believe this equation

$$I_0/I = 1 + K_{SV}[Q] + k_{ET}\tau_f[Q] \tag{3}$$

is consistent with a static-quencher situation, which can be described as a continuous quenching process for the Green master equation derived model.[21] In this equation K_{SV} is the static Stern−Volmer constant, [Q] the concentration of quencher, k_{ET} the rate of energy transfer, and τ_f the lifetime of the nonquenched fluorophore. In this case, the K_{SV} term accounts for fluorescence loss only for the static, metal-bound receptor sites, and the k_{ET} term accounts for energy transfer from excitons that are not immediately adjacent to the metal-bound receptor site. This equation takes on a more specific form dependent upon the energy-transfer mechanism: trivial, Förster (dipole−dipole), or Dexter (orbital overlap) mechanism.[31] Common to all these mechanisms is the importance of the donor−acceptor distance, though the specific dependence on this term differs for each of these mechanisms. We have chosen to represent the donor−acceptor distance generically, as shown in eq 4, where r is the donor acceptor distance, l is the average monomer length, and [receptor] is the polymer concentration in terms of pendant receptors.

$$r = l([\text{receptor}]/[Q]) \tag{4}$$

To appropriately fit the observed Stern−Volmer data by this modified equation, the mechanism of energy transfer must be known. Since the trivial mechanism has no distance dependence it cannot account for the loading dependence observed in Figure 6 and will not be considered further here. We have fit both Förster and Dexter energy-transfer mechanisms individually to our Stern−Volmer analysis. With use of a Förster-derived rate based on dipole−dipole energy transfer,[31] the rate k_{ET} is given by eq 5, where τ_f is the lifetime of the donor species and R_0 is

$$k_{ET} = \frac{1}{\tau_f}\left(\frac{R_0}{r}\right)^6 \tag{5}$$

the distance at which energy transfer between the donor and the acceptor is 50% likely to occur, also known as the critical distance (eq 6). Adapting the second term of our Stern−Volmer

$${R_0}^6 = \frac{(8.8 \times 10^{-25})\kappa^2\phi_D}{n^4}\int_0^\infty F_D(\nu)\epsilon_A(\nu)\frac{d\nu}{\nu^4} \tag{6}$$

equation to take into account Förster energy transfer and our distance approximation, we are left with eq 7. One should note that in this form, the loading dependence can be controlled,

$$I_0/I = 1 + K_{SV}[Q] + \left(\frac{R_0}{r}\right)^6[Q] \tag{7}$$

leaving a two-variable fit for K_{SV} and R_0. Of these, the Stern−Volmer constant K_{SV} can be determined from the linear portion of the emission quenching data at very low concentrations of the quencher (Figure 4), where the energy-transfer term (either Förster or Dexter) will be infinitesimally small. The Förster enhancement can thus be fit only to R_0 and optimized by minimizing the square of the sum of residuals (SSR).

Similarly, Dexter energy transfer[31] can be expressed in Stern−Volmer form as shown in eq 8, where K is a constant in units of energy, L is also a constant value called the effective average

$$k_{ET} = (2\pi/\hbar)K^2 \exp(-2R/L)\int f_D(\nu)f_A(\nu)\, d\nu \tag{8}$$

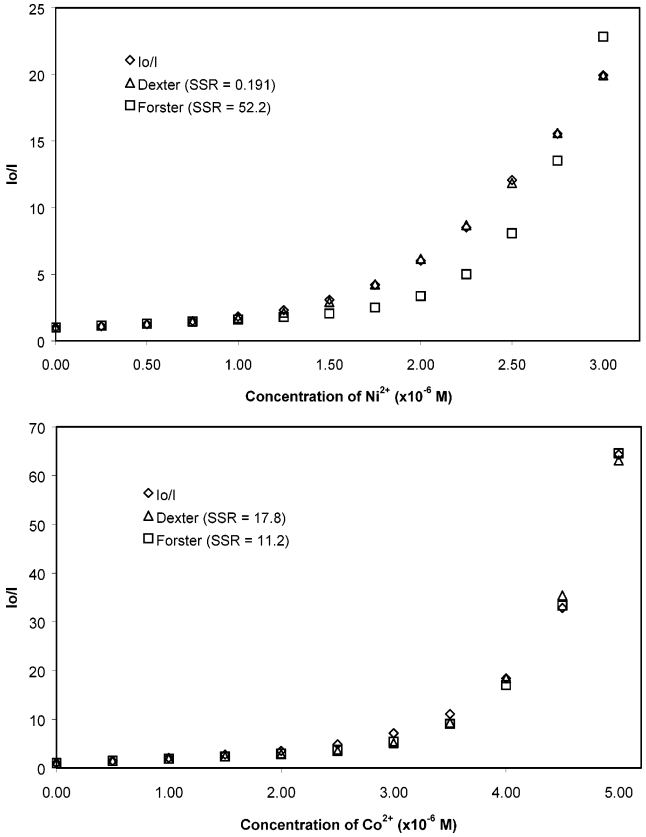

Figure 7. Comparison of Förster and Dexter energy-transfer enhancements in the quenching of 5.00×10^{-6} M **ttp-PPETE** by (a) Ni^{2+} and (b) Co^{2+} ions. In each fit, diamonds represent raw data, squares the calculated fit for the Förster mechanism, and triangles the calculated fit for the Dexter mechanism, with SSR values in parentheses.

Bohr radius, $f_A(\nu)$ and $f_D(\nu)$ are the acceptor absorbance and donor emission oscillator strengths, respectively, and r is the donor−acceptor distance. We simplify this expression by combining the integral expression and other constants into the K-squared term (eq 9),[32] and fit this equation using the same relationship for r as shown for the Förster expression (eq 4).

$$K'^2 = K^2(2\pi/\hbar)\int f_D(\nu)f_A(\nu)\,d\nu \qquad (9)$$

The Dexter form of the equation can be fit to two terms, K' and L, as shown in eq 10, and optimized by minimizing the SSR.

$$I_0/I = 1 + K_{SV}[Q] + \tau_f[Q]K'^2\exp(-2r/L) \qquad (10)$$

Application of our model to the Stern−Volmer quenching of **ttp-PPETE** by Co^{2+} and Ni^{2+} ions is shown in Figure 7, panels a and b, respectivel,y and the numerical results are shown in Table 2, along with SSR values for each method. From each plot one can observe that a different curvature for energy-transfer enhancement is observed depending on whether Förster or Dexter energy transfer is involved. The cobalt quenching data demonstrate a curvature consistent with a Forster-type enhancement, while the nickel quenching data are more consistent with a Dexter-type enhancement. From the combined Stern−Volmer plot in Figure 4, one also notes that the nickel-quenching plot achieves a higher degree of quenching of **ttp-PPETE** than cobalt at similar metal ion concentrations. These preferences for one energy-transfer mechanism over another are marked by orders of magnitude differences in the SSR of the fits, Table 2. Thus we conclude that the source of the observed nonlinearity is due to variations in the energy-transfer rate along the polymer backbone.

TABLE 2: Stern−Volmer Constants and Energy-Transfer Parameters for Fits of Quenching Data for 5.00×10^{-6} M ttp-PPETE in THF

analyte	$K_{sv}{}^a$ ($\times 10^5$)	$R_0{}^{b,c}$	K'^c ($\times 10^3$)	L^b
Ni^{2+}	5.91	22.9 (52.2)	12.0 (0.191)	1.57
Co^{2+}	9.06	15.1 (11.2)	65.8 (17.8)	0.41
Cu^{2+}	2.01	22.1 (17.6)	11.7 (30.0)	0.49
Fe^{2+}	1.49	14.2 (999)	5.81 (1.35)	3.59

[a] In M^{-1}. [b] In monomer unit lengths, l. [c] SSR values in parentheses.

At low concentrations of quenchers, the differences between the K_{SV} values for each of the transition metal analytes is not as pronounced, as the energy-transfer enhancements are small relative to static quenching, Figure 4. The magnitude of the differences in the static K_{SV} values for the different metals was somewhat unexpected. Previous studies on the binding of terpyridine to transition metals have shown significant variations of a few orders of magnitude for the binding of different metals.[17] This suggests that the binding equilibrium is not a factor in the nonlinear quenching behavior as noted above. The specific role that the binding equilibrium may play in the quenching process is the subject of further investigation.[30]

At high quencher concentrations where the energy-transfer component dominates, one would expect the fluorescence lifetime to decrease. This is easily seen if you simplify the lifetime τ_f as shown in eq 11. As the rate of energy transfer increases, the lifetime must decrease. We were not able to confirm this by single-photon counting lifetimes at high quencher concentrations. The fluorescence was so weak that

$$\tau_f = \frac{1}{k_r + k_{nr} + k_{ET}} \qquad (11)$$

the lifetime measurements were subject to significant error. At low quencher concentrations, where the rate of energy transfer is still small, the fluorescence observed is largely unperturbed by the loading of quencher analytes as expected.

Conclusions

Understanding the quenching dynamics of receptor functionalized fluorescent conjugated polymers is critical to the design of chemosensory materials. Using Stern−Volmer analysis, we have shown that a combination of static and dynamic processes contributes to the quenching process in the **ttp-PPETE** system in the presence of transition metal ions in solutions. The nonlinear behavior observed was attributed to a combination of static quenching and an energy-transfer enhancement of the quenching as a result of energy migration along the polymer backbone. On the basis of this model, it was demonstrated that different energy-transfer mechanisms exist, Dexter vs Förster, as a function of the chemical identity of the analyte. Through careful tuning of the receptor interactions with both the polymer backbone and the analyte it may therefore be possible to create a more selective system for future chemosensory polymers.

Acknowledgment. The authors wish to thank Brian King, Scott Gilje, and Dr. Stanley K. Madan for additional work and discussion about this project. The authors also thank Dr. John Van Houten and Dr. Alistair Lees for useful discussions pertaining to the Stern-Volmer model. We would also like to thank Dr. Troxler and Dr. Rubtsov for their time and expertise with experiments performed at the NIH RLBL (NIH grant P41 RR01348). Funding was graciously supplied through grants from the National Institute of Health (NIH grant 1R15ES10106-01) and the Research Foundation at the State University of New York at Binghamton.

References and Notes

(1) McQuade, D. J.; Pullen, A. E.; Swager, T. M. *Chem. Rev.* **2000**, *100*, 2357.

(2) Prodi, L.; Bolleta, F.; Montalti, M.; Zaccheroni, N. *Coord. Chem. Rev.* **2000**, *205*, 59.

(3) Swager, T. M. *Acc. Chem. Res.* **1998**, *31*, 201.

(4) (a) Wang, B.; Wasielewski, M. R. *J. Am. Chem. Soc.* **1997**, *199*, 112. (b) Chen, L.-X.; Jäger, W. J. H.; Gosztola, D. J.; Neimczyk, M. P.; Wasielewski, M. R. *J. Phys. Chem.* **2000**, *104*, 1950. (c) Chen, L.-X.; Jäger, W. J. H.; Gosztola, D. J.; Neimczyk, M. P.; Wasielewski, M. R. *Synth. Met.* **2001**, *116*, 229.

(5) (a) Zotti, G.; Zecchin, S.; Schiavon, G.; Berlin, A.; Penso, M. *Chem. Mater.* **1999**, *11*, 3342. (b) Bouachrine, M.; Lère-Porte, J.-P.; Moreau, J. J. E.; Serein-Spirau, F.; Torreilles, C. *J. Mater. Chem.* **2000**, *10*, 263. (c) Bangcuyo, C. G.; Rampey-Vaughn, M. E.; Quan, L. T.; Angel, S. M.; Smith, M. D.; Bunz, U. H. F. *Macromolecules* **2002**, *35*, 1563.

(6) Zhu, S. S.; Swager, T. M. *J. Am. Chem. Soc.* **1997**, *199*, 112568.

(7) McQuade, D. T.; Hegedus, A. H.; Swager, T. M. *J. Am. Chem. Soc.* **2000**, *122*, 12389.

(8) (a) Chen, L.; McBranch, D. W.; Wang, H.-L.; Helgeson, R.; Wudl, F.; Whitten, D. G. *Proc. Natl. Acad. Sci. U.S.A.* **1999**, *96*, 12287. (b) Chen, L.; Su, X.; McBranch, D. W.; Whitten, D. G. *J. Am. Chem. Soc.* **2000**, *122*, 9302. (c) Jones, R. M.; Bergstedt, T. S.; McBranch, D. W.; Whitten, D. G. *J. Am. Chem. Soc.* **2001**, *123*, 6726.

(9) (a) Wang, J.; Wang, D.; Miller, E. K.; Moses, D.; Bazan, G. C.; Heeger, A. J. *Macromolecules* **2000**, *33*, 5153. (b) Wang, D.; Wang, J.; Moses, D.; Bazan, G. C.; Heeger, A. J. *Langmuir* **2001**, *17* (4), 1262.

(10) Jiang, B.; Sahay, S.; Jones, W. E. *Mater. Res. Soc. Symp. Proc.* **1998**, *488*, 671.

(11) Zhang, Y.; Murphy, C. B.; Jones, W. E. *Macromolecules* **2002**, *35*, 630.

(12) Jones, W. E.; Murphy, C. B.; Zhang, Y.; Ferry, V.; Gilje, S. In *Advanced Environmental Sensing Technology II*; Vo-Dinh, T., Büttgenbach, S., Eds.; Proceedings of the SPIE; 2002; Vol. 4576, pp 10−18.

(13) U.S. EPA, Fed. Regist. 1973.

(14) Department of Health and Human Services, Fed. Regist. 1996, 14419.

(15) Pang, Y.; Li, J.; Barton, T. J. *J. Mater. Chem.* **1998**, *8*, 1687.

(16) In the context of a review of Poly(aryleneethynylenes): Bunz, U. H. F. *Chem. Rev.* **2000**, *100*, 1605.

(17) Martell, A. E.; Smith, R. M. *Critical Stability Constants*; Plenum Press: New York and London, 1974; Vol. 5.

(18) (a) Kilp, T.; Guillet, J. E. *Macromolecules* **1981**, *14*, 1680. (b) Winnik, M. A.; Disanayaka, B.; Peckan, O.; Croucher, M. D. *J. Colloid Interface Sci.* **1990**, *139*, 251. (c) Fox, H. H.; Fox, M. A. *Macromolecules* **1995**, *28*, 4570. (d) Yang, J.; Winnik, M. A.; Ylitalo, D.; DeVoe, R. J. *Macromolecules* **1996**, *29*, 7055.

(19) (a) Webber, S. E.; Avots-Avotins, P. E.; Deumiè, M. *Macromolecules* **1981**, *14*, 105. (b) Hargreaves, J. S.; Webber, S. E. *Macromolecules* **1984**, *17*, 235. (c) Bai, F.; Chang, C.-H.; Webber, S. E. Alternating Copolymers of 2-Vinylnaphthalene and Methacrylic Acid in Aqueous Solution. In *Photophysics of Polymers*; Hoyle, C. E., Torkelson, J. M., Eds.; ACS Symp. Ser. 358; American Chemical Society: Washington, DC, 1987; pp 384−411.

(20) (a) Grazulevicius, J. V.; Soutar, I.; Swanson, L. *Macromolecules* **1998**, *31*, 4280. (b) De, A. K.; Ganguly, A. K. *J. Lumin.* **2001**, *92*, 255.

(21) Lakatos-Lindenberg, K.; Hemenger, R. P.; Pearlstein, R. M. *J. Chem. Phys.* **1972**, *56*, 4852.

(22) Fitzgibbon, P. D.; Frank, C. W. *Macromolecules* **1982**, *15*, 733.

(23) Webber, S. E. *Chem. Rev.* **1990**, *90*, 1469.

(24) Itoh, Y.; Kamioka, K.; Webber, S. E. *Macromolecules* **1989**, *22*, 2851.

(25) (a) Jones, R. M.; Bergestedt, T. S.; Buscher, C. T.; McBranch, D. W.; Whitten, D. G. *Langmuir* **2001**, *17*, 2568. (b) Lu, L. D.; Helgeson, R.; Jones, R. M.; McBranch, D. W.; Whitten, D. G. *J. Am. Chem. Soc.* **2002**, *124*, 482.

(26) (a) Holtom, G. R. Time-resolved Laser Spectroscopy in Biochemistry II. In *SPIE Proc. Ser.* **1990**, *1204*, 2−12. (b) De Paula, J. C.; Liefschitz, A.; Hinsley, S.; Lin, W.; Chopra, K.; Long, K.; Williams, S. A.; Betts, S.; Yocum, C. F. *Biochemistry* **1994**, *33*, 1455.

(27) Billo, E. J. *Excel for Chemists*; Wiley-VCH: New York, 2001.

(28) Lakowicz, J. R. *Principles of Fluorescence Spectroscopy*; Plenum Press: New York and London, 1983.

(29) Constable, E. C.; Phillips, D.; Raithby, P. R. *Inorg. Chem. Commun.* **2002**, *5*, 519.

(30) Murphy, C. B.; Pluchino, K.; Noriega, T. R.; Zavilij, P.; Jones, W. E. *J. Fluorescence*. Submitted for publication.

(31) Guillet, J. *Polymer Photophysics and Photochemistry*; Cambridge University Press: Cambridge, UK, 1985.

(32) This keeps the Dexter expression analogous to the Förster expression, where the principal constant of the latter, R_0, includes the overlap integral.